Advances in Reliability, Safety and Security, Part 8 – Kołowrocki, Magryta-Mut (eds.)
© 2024 Polish Safety and Reliability Association, Gdynia, ISBN 978-83-68136-20-3 (printed), ISBN 978-83-68136-07-4 (electronic)

Advances in Reliability, Safety and Security

ESREL 2024
Monograph Book Series

Risk Coupling Analysis On Ship Path Entering Into Port: Case Study In Shenzhen Port

Cunlong Fan[a], Bing Wang[b], Yamin Huang[c,d,e], Yuhui Qiu[a]

[a]*College of Transportation & Communications, Shanghai Maritime University, Shanghai, China*
[b]*School of Navigation, Wuhan University of Technology, Wuhan, China*
[c]*State Key Laboratory of Maritime Technology and Safety, Wuhan University of Technology, Wuhan, China*
[d]*National Engineering Research Center for Water Transport Safety, Wuhan University of Technology, Wuhan, China*
[e]*Intelligent Transportation Systems Research Center, Wuhan University of Technology, Wuhan, China*

Abstract

Ship traffic is heavy in the port waters, especially to ports located in the estuary. Shenzhen port has been one of world-class ports in the estuary of Pearl River Delta. High volume of traffic indicates the active development of regional society but also potential navigation risk. This study aims to quantitative risk coupling analysis on the path of ship entering into a port. To this end, accidents, i.e., grounding, are collected and the failure modes involved in an accident are identified and classified into five types of risk factors, i.e., human-related, organization-related, ship-related, environment-related, and technology-related. A path of ship entering into a port is established, including three parts, the open sea, channel, and the berth. Based on historical data, the risk coupling values in the part of channel and berth are quantified using the N-K model. Then, based on the developed path, the risk coupling value of a ship path is generated. The results may be used to support decision-making onboard.

Keywords: risk coupling analysis, ship path, Shenzhen port, grounding

1. Introduction

Port is a pivotal node in the international trade, supply chain, and the development of port-city (Chen et al., 2022; Qu et al., 2023). For example, the Shenzhen port, China, has been a significant driver for the Shenzhen city development (Gan et al., 2022; Wang et al., 2022). Moreover, the Shenzhen port has been one of world-class ports in the Guangdong-Hong Kong-Macao Greater Bay Area from the view of container throughputs released in Lloyd’s List’s seaport ranking 2011-2019. This port, as a hub for linking domestic and international markets, has played an important role in the development of regional economy (Fu et al., 2023; Kong and Liu, 2021; Zhong et al., 2023). For example, the Shenzhen port is home to 40 shipping companies that have launched around 239 international container routes (Gan et al., 2022). In such international port, the traffic is also busy (Mou et al., 2019), which leads to the port area, e.g., channel, anchorage, and berth that the ship entering and leaving as the place with high frequency of ship accidents (Aalberg et al., 2022; Zhao et al., 2022). Ship accidents in the port area is highly likely to disrupt the continuous production of port, e.g., m/t Angel, in July 2023, sank outside the Port of Kaohsiung, leading a large number of containers to fall into the sea, which affected the safety of the waterway (Marineinsight, 2023).

Learning from ship accidents in port waters could shed light on navigational risk management in these areas. Ship accidents or incidents in the port waters have been investigated by many researchers. For example, Mou et al. (2019) proposed a framework of safety indexes to evaluate the risk level in busy waterways according to the accident severity, fatality rate and special indicators of maritime transportation. Hua et al. (2021) used Fault Tree Analysis to analyze the causation factors of the hazardous cargo explosion at Tianjin Port of China. Wang et al. (2021) analyzed the dependency and interdependency among the risk factors influencing port state control inspection. Yang et al. (2021) used Bayesian network-based Technique for Order Preference by Similarity to Ideal Solution to aid dynamic port state control detention risk control decision. Fan et al. (2022b) analyzed impacts of dynamic inspection records on port state control efficiency using Bayesian network. They found that high levels of safety and labor condition related defects significantly increase the accident rate. Montewka et al. (2022) presented a generic framework evaluating accident susceptibility index for ships carrying passengers. Liu et al. (2022) used a data training technique and the newest port state control data to improve the usage of Bayesian network to assess detention risk to a point where risk factors are identified, interrelationships among the factors are analyzed and prior probability training based on big data is obtained more easily. Ma et al. (2023) proposed a hybrid method integrating the Functional Resonance Analysis Method, fuzzy set theory, and risk matrix to quantitatively assess the risks triggered by failure coupling links between upstream and downstream functions in the hazardous chemicals maritime transportation system.

However, few study devote to risk coupling effects of ship entering into port waters. This research aims to fill this gap. To this end, a framework is proposed including three steps. Taking ship from the open sea to enter a berth in the west of Shenzhen port as case study, this study listed a system comprised by two sub-systems, considering the geographic condition, operational process. The research results could provide risk coupling information for decision-makers, especially the crew onboard.

2. Framework and methodology

Assuming that a system is used to describe the process of ship entering into a port, including several sub-systems, e.g., the channel, anchorage, berth. In **Step 1**, ship accidents occurred in the port area are collected and analyzed by a systematic accident analysis model, i.e., 24Model proposed by Fu et al. (2020). And statistical analysis is conducted to calculate the risk coupling probabilities in coupling scenarios involving multiple risk types. In **Step 2**, we firstly calculated the risk coupling values (RCVs) of sub-systems in a system. In this step, the N-K model proposed by Kauffman and Weinberger (1989) is employed to calculate the RCVs. In **Step 3**, based on the system structure, the generated RCVs were used to generate the RCV of the system. The sub-systems in a system are channel, anchorage, and berth, which are assumed to be mutual independent. In this context, the RCV of a system is a product of the RCVs of the sub-systems.

3. Case study

3.1. Data source

3.1.1. Data source

The historical accident data in this study is grounding in the west of Shenzhen port collected from the Shenzhen Maritime Safety Administration (MSA). The data from January 2003 to July 2014 is collected from the Vessel Traffic Service (VTS) center of Shenzhen MSA, while the data from August 2014 to December 2022 is from the website of Shenzhen MSA. In total, 98 grounding cases occurred during the last 20 years are the data sample for this study.

According the position information in the 98 grounding data sample, there were 66 cases ran aground in channel, 17 in anchorage and 15 in berth. To minimize such difference in these three areas, we divided the whole data sample into two sub-samples for channel, anchorage or berth. There two areas are sub-systems in the following two cases. From the description in the data sample, using 24Model identified 15 general FMs that presented in Fan et al. (2022a), and shown in Table 1.

Table 1. Classification on failure modes leading to grounding in the west of Shenzhen port.

Type	Human (H)	Organization (O)	Ship (S)	Environment (E)	Technology (T)
Failure mode	Improper assessment of ship position (H1)	Inappropriate/ineffective Maintenance (O1)	Ineffective use of technology (S1)	Inappropriate stowage of cargo (E1)	Mishandling (T1)
	Inadequate lookout (H2)	Overloading (O2)	Insufficient anticipation of nautical conditions (S2)	Failure in Communication (E2)	Poor management of voyage plan (T2)
	Inadequate training in personal quality or sample for decision Making (H3)	Under-manning (O3)	Main engine failure (S3)	Weather/other environmental factors (E3)	Rule violation (T3)

3.1.2. Risk coupling probabilities in two areas

To an accident in the data sample, we assigned 0 or 1 to according to the classification map, i.e., Table 1, between failure modes and type of risk factors. For example, if an accident in the sub-sample of channel involves only organization-related factors, then the state of H, O, S, E, T of this case is marked by 01000, which is a combination of states of these five types of risk factors. Repeat this operation for the rest, the marks of states of H, O, S, E, T in the sub-sample of channel are generated and used to count the number and the probability of each combination of these five risk types. The counting results on grounding in channel are shown in Table 2. For example, there are 2 cases marked by 10000, then the probability of this combination of these five types of risk factors is about 0.0303. Similarly, the results in the sub-sample of anchorage are generated.

Table 2. Number and probability of these five risk types combination in the counted grounding occurred in Channel.

Single Factor	Number (State of H, O, S, E, T)	0 (00000)	2 (10000)	3 (01000)	1 (00100)	1 (00010)	1 (00001)
	P_{hoset}	P_{00000} = 0	P_{10000} = 0.0303	P_{01000} = 0.0454	P_{00100} = 0.0152	P_{00010} = 0.0152	P_{00001} = 0.0152
Two Factors	Number (State of H, O, S, E, T)	0 (11000)	11 (10100)	2 (10010)	7 (10001)	2 (01100)	1 (01010)
	P_{hoset}	P_{11000} = 0	P_{10100} = 0.1666	P_{10010} = 0.0303	P_{10001} = 0.106	P_{01100} = 0.0303	P_{01010} = 0.0152
	Number (State of H, O, S, E, T)	1 (01001)	2 (00110)	4 (00101)	2 (00011)	NA	NA
	P_{hoset}	P_{01001} = 0.0152	P_{00110}= 0.0303	P_{00101}= 0.0605	P_{00011}= 0.0303	NA	NA
Three Factors	Number (State of H, O, S, E, T)	1 (11100)	1 (11010)	0 (11001)	3 (10110)	3 (10101)	2 (10011)
	P_{hoset}	P_{11100}= 0.0152	P_{11010}= 0.0152	P_{11001} = 0	P_{10110} = 0.0455	P_{10101} = 0.0455	P_{10011} = 0.0303
	Number (State of H, O, S, E, T)	0 (01110)	0 (01101)	0 (01011)	1 (00111)	NA	NA
	P_{hoset}	P_{01110} = 0	P_{01101} = 0	P_{01011} = 0	P_{00111} = 0.0152	NA	NA
Four Factors	Number (State of H, O, S, E, T)	4 (11110)	2 (11101)	1 (11011)	8 (10111)	0 (01111)	NA
	P_{hoset}	P_{11110} = 0.0605	P_{11101} = 0.0303	P_{11011} = 0.0152	P_{10111} = 0.1211	P_{01111} = 0	NA

Five Factors	Number (State of H, O, S, E, T)	0 (11111)	NA	NA	NA	NA	NA
	P_{hoset}	P_{11111} = 0	NA	NA	NA	NA	NA

Based on Table 2 and the N-K model algorithm, the risk coupling probabilities in given scenario in these two sub-samples are generated. Due to the limited space, the results in the sub-sample of channel are shown in Tables 3-6.

Table 3 Risk coupling probability of single risk type in Channel.

P_h	P_o	P_s	P_e	P_t
$P_{0....}$ = 0.2880	$P_{.0...}$ = 0.7575	$P_{..0..}$ = 0.3638	$P_{...0.}$ = 0.5757	$P_{....0}$ = 0.5152
$P_{1....}$ = **0.7120**	$P_{.1...}$ = **0.2425**	$P_{..1..}$ = 0.6362	$P_{...1.}$ = 0.4243	$P_{....1}$ = 0.4848

Table 4 Risk coupling probability of two risk types in Channel.

P_{ho}	P_{hs}	P_{he}	P_{ht}	P_{os}
$P_{00...}$ = 0.1819	$P_{0.0..}$ = 0.1365	$P_{0..0.}$ = 0.1818	$P_{0...0}$ = 0.1516	$P_{.00..}$ = 0.2576
$P_{01...}$ = 0.1061	$P_{0.1..}$ = 0.1515	$P_{0..1.}$ = 0.1062	$P_{0...1}$ = 0.1364	$P_{.01..}$ = 0.4999
$P_{10...}$ = 0.5756	$P_{1.0..}$ = 0.2273	$P_{1..0.}$ = 0.3939	$P_{1...0}$ = 0.3636	$P_{.10..}$ = 0.1062
$P_{11...}$ = 0.1364	$P_{1.1..}$ = **0.4847**	$P_{1..1.}$ = 0.3181	$P_{1...1}$ = 0.3484	$P_{.11..}$ = 0.1363
P_{oe}	P_{ot}	P_{se}	P_{st}	P_{et}
$P_{.0.0.}$ = 0.4393	$P_{.0..0}$ = 0.3334	$P_{..00.}$ = 0.2121	$P_{..0.0}$ = 0.1516	$P_{...00}$ = 0.3030
$P_{.0.1.}$ = 0.3182	$P_{.0..1}$ = 0.4241	$P_{..01.}$ = 0.1517	$P_{..0.1}$ = 0.2122	$P_{...01}$ = 0.2727
$P_{.1.0.}$ = 0.1364	$P_{.1..0}$ = 0.1818	$P_{..10.}$ = 0.3636	$P_{..1.0}$ = 0.3636	$P_{...10}$ = 0.2122
$P_{.1.1.}$ = 0.1061	$P_{.1..1}$ = **0.0607**	$P_{..11.}$ = 0.2726	$P_{..1.1}$ = 0.2726	$P_{...11}$ = 0.2121

Table 5 Risk coupling probability of three risk types in Channel.

P_{hos}	P_{hoe}	P_{hot}	P_{hse}	P_{hst}
$P_{000..}$ = 0.0607	$P_{00.0.}$ = 0.0909	$P_{00..0}$ = 0.0607	$P_{0.00.}$ = 0.0758	$P_{0.0.0}$ = 0.0758
$P_{001..}$ = 0.1212	$P_{00.1.}$ = 0.0910	$P_{00..1}$ = 0.1212	$P_{0.01.}$ = 0.0607	$P_{0.0.1}$ = 0.0607
$P_{010..}$ = 0.0758	$P_{01.0.}$ = 0.0909	$P_{01..0}$ = 0.0909	$P_{0.10.}$ = 0.1060	$P_{0.1.0}$ = 0.0758
$P_{011..}$ = 0.0303	$P_{01.1.}$ = 0.0152	$P_{01..1}$ = 0.0152	$P_{0.11.}$ = 0.0455	$P_{0.1.1}$ = 0.0757
$P_{100..}$ = 0.1969	$P_{10.0.}$ = 0.3484	$P_{10..0}$ = 0.2727	$P_{1.00.}$ = 0.1363	$P_{1.0.0}$ = 0.0758
$P_{101..}$ = 0.3787	$P_{10.1.}$ = 0.2272	$P_{10..1}$ = 0.3029	$P_{1.01.}$ = 0.0910	$P_{1.0.1}$ = 0.1515
$P_{110..}$ = 0.0304	$P_{11.0.}$ = 0.0455	$P_{11..0}$ = 0.0909	$P_{1.10.}$ = 0.2576	$P_{1.1.0}$ = 0.2878
$P_{111..}$ = 0.1060	$P_{11.1.}$ = 0.0909	$P_{11..1}$ = 0.0455	$P_{1.11.}$ = **0.2271**	$P_{1.1.1}$ = 0.1969
P_{het}	P_{ose}	P_{ost}	P_{oet}	P_{set}
$P_{0..00}$ = 0.0909	$P_{.000.}$ = 0.1515	$P_{.00.0}$ = 0.0758	$P_{.0.00}$ = 0.2121	$P_{..000}$ = 0.0757
$P_{0..01}$ = 0.0909	$P_{.001.}$ = 0.1061	$P_{.00.1}$ = 0.1818	$P_{.0.01}$ = 0.2272	$P_{..001}$ = 0.1364
$P_{0..10}$ = 0.0607	$P_{.010.}$ = 0.2878	$P_{.01.0}$ = 0.2576	$P_{.0.10}$ = 0.1213	$P_{..010}$ = 0.0759
$P_{0..11}$ = 0.0455	$P_{.011.}$ = 0.2121	$P_{.01.1}$ = 0.2423	$P_{.0.11}$ = 0.1969	$P_{..011}$ = 0.0758
$P_{1..00}$ = 0.2121	$P_{.100.}$ = 0.0606	$P_{.10.0}$ = 0.0758	$P_{.1.00}$ = 0.0909	$P_{..100}$ = 0.2273
$P_{1..01}$ = 0.1818	$P_{.101.}$ = 0.0456	$P_{.10.1}$ = 0.0304	$P_{.1.01}$ = 0.0455	$P_{..101}$ = 0.1363
$P_{1..10}$ = 0.1515	$P_{.110.}$ = 0.0758	$P_{.11.0}$ = 0.1060	$P_{.1.10}$ = 0.0909	$P_{..110}$ = 0.1363
$P_{1..11}$ = 0.1666	$P_{.111.}$ = 0.0605	$P_{.11.1}$ = 0.0303	$P_{.1.11}$ = **0.0152**	$P_{..111}$ = 0.1363

Table 6 Risk coupling probability of four risk types in Channel.

P_{hose}	P_{host}	P_{hoet}	P_{hset}	P_{oset}
$P_{0000.}$ = 0.0152	$P_{000.0}$ = 0.0152	$P_{00.00}$ = 0.0152	$P_{0.000}$ = 0.0454	$P_{.0000}$ = 0.0303
$P_{0001.}$ = 0.0455	$P_{000.1}$ = 0.0455	$P_{00.01}$ = 0.0757	$P_{0.001}$ = 0.0304	$P_{.0001}$ = 0.1212
$P_{0010.}$ = 0.0757	$P_{001.0}$ = 0.0455	$P_{00.10}$ = 0.0455	$P_{0.010}$ = 0.0304	$P_{.0010}$ = 0.0455
$P_{0011.}$ = 0.0455	$P_{001.1}$ = 0.0757	$P_{00.11}$ = 0.0455	$P_{0.011}$ = 0.0303	$P_{.0011}$ = 0.0606
$P_{0100.}$ = 0.0606	$P_{010.0}$ = 0.0606	$P_{01.00}$ = 0.0757	$P_{0.100}$ = 0.0455	$P_{.0100}$ = 0.1818
$P_{0101.}$ = 0.0152	$P_{010.1}$ = 0.0152	$P_{01.01}$ = 0.0152	$P_{0.101}$ = 0.0605	$P_{.0101}$ = 0.1060
$P_{1000.}$ = 0.1363	$P_{100.0}$ = 0.0606	$P_{10.00}$ = 0.1969	$P_{1.000}$ = 0.0303	$P_{.1000}$ = 0.0454
$P_{1001.}$ = 0.0606	$P_{100.1}$ = 0.1363	$P_{10.01}$ = 0.1515	$P_{1.001}$ = 0.1060	$P_{.1001}$ = 0.0152
$P_{1100.}$ = 0.0000	$P_{110.0}$ = 0.0152	$P_{11.00}$ = 0.0152	$P_{1.100}$ = 0.1818	$P_{.1100}$ = 0.0455
$P_{1101.}$ = 0.0304	$P_{110.1}$ = 0.0152	$P_{11.01}$ = 0.0303	$P_{1.101}$ = 0.0758	$P_{.1101}$ = 0.0303
$P_{1010.}$ = 0.2121	$P_{101.0}$ = 0.2121	$P_{10.10}$ = 0.0758	$P_{1.010}$ = 0.0455	$P_{.1010}$ = 0.0304
$P_{1011.}$ = 0.1666	$P_{101.1}$ = 0.1666	$P_{10.11}$ = 0.1514	$P_{1.011}$ = 0.0455	$P_{.1011}$ = 0.0152
$P_{0110.}$ = 0.0303	$P_{011.0}$ = 0.0303	$P_{01.10}$ = 0.0152	$P_{0.110}$ = 0.0303	$P_{.0110}$ = 0.0758
$P_{0111.}$ = 0.0000	$P_{011.1}$ = 0.0000	$P_{01.11}$ = 0.0000	$P_{0.111}$ = 0.0152	$P_{.0111}$ = 0.1363
$P_{1110.}$ = 0.0455	$P_{111.0}$ = 0.0757	$P_{11.10}$ = 0.0757	$P_{1.110}$ = 0.1060	$P_{.1110}$ = 0.0605
$P_{1111.}$ = 0.0605	$P_{111.1}$ = 0.0303	$P_{11.11}$ = 0.0152	$P_{1.111}$ = **0.1211**	$P_{.1111}$ = **0.0000**

From Table 2, the number of grounding involving two risk types is the highest in the sub-sample of channel. For example, for these grounding cases involving three risk types, two combinations of these three types of risk factors, i.e., the human-related, ship-related, and environment-related, with the state marked by 10110, the human-related, ship-related, and technology-related, with the state marked by 10101, are larger than others in the frequency. Except for the mark of 00000, there are some marks with 0 in number and probability, e.g., 11000, 11001, 01111, 11111.

Based on risk coupling probabilities, we calculated RCVs in the sub-samples of the two areas within the two to five risk types coupling scenarios, using the N-K algorithm. The results of RCVs of these scenarios in the sub-samples of the two areas are shown in Fig. 1. For example, in five risk types coupling scenario, the risk coupling values in the sub-sample of anchorage or berth is larger than that of channel. These two risk coupling values, i.e., 0.4569 in the channel, and 1.1776 in anchorage or berth.

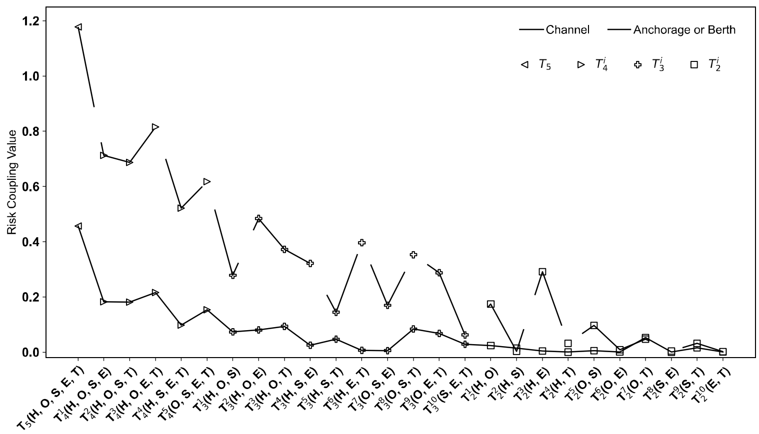

Fig. 1. Risk coupling values in the sub-samples of two areas.

3.2. A case to enter into the west of Shenzhen port

Main waterways in the west of Shenzhen port is simplified and shown in Fig. 2. From the view of seafarers, there are two main paths from the open sea to the berth in the west of Shenzhen port. One is from the Tonggu channel, another from the Longgu channel. Before entering the berth in the western coast of Shenzhen port, a public channel is required. The path in this case begins at open sea, passes through the Tonggu or Longgu channel, and Public channel, and finally arrives at the berth. Fig. 3 reflects this process, with sub-system 1 as the channel, sub-system 2 as the berth.

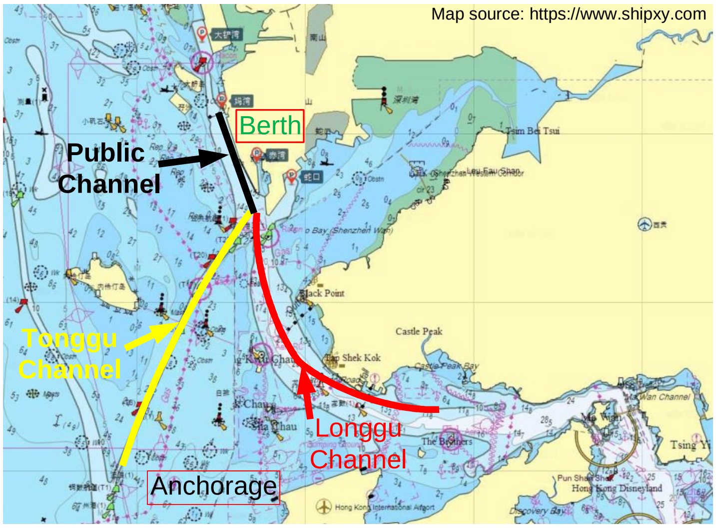

Fig. 2 Main paths to the west of Shenzhen port waters.

In this case, a voyage plan entering into the west coast of Shenzhen port, begins from the open sea, passes through the Tonggu or Longgu channel, and Public channel, and finally arrives at the berth. Fig. 3 presents the process of the case, including two sub-systems, i.e., sub-system 1, channel; sub-system 2, berth. Then, according to the interval valued risk coupling probabilities in Section 3.1.2 and the N-K algorithm, we calculated the risk coupling values in the case with different number of risk types in these two sub-systems.

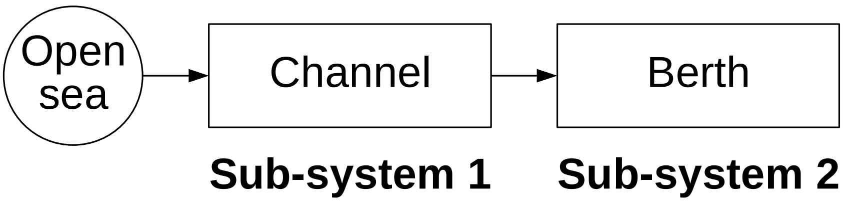

Fig. 3. A structure of entering the west coast of Shenzhen port.

Table 7 shows the results of 26 assumed scenarios in case of five risk types in sub-system 1 and multiple risk types in sub-system 2. From Table 7, we can find that as the risk types in the sub-system 2 decreases, the RCVs of the whole system also decreases. The maximum RCV of the whole system is at 0.5380 when both of two sub-systems involve these five types of risk, while the minimum RCV of the whole system is at 0.0006 when sub-system 2 involves two types of risk, i.e., environment and technology, in condition that sub-system 1 involves these five types of risk. However, there are RCVs of certain scenarios when the sub-system 2 involves two risk types larger than that of certain scenarios when the sub-system 2 involves three risk types. For example, in the case that the sub-system 2 involves two risk types, i.e., human and environment, the RCV of the whole system is larger than that when the sub-system 2 involves three risk types, i.e., ship, environment, and technology.

Table7. Risk coupling values in 26 scenarios.

No.	RCV of the Sub-system 1	RCV of the Sub-system 2	RCV of the whole system
1	$T_5(H,O,S,E,T) = 0.4569$	$T_5(H,O,S,E,T) = 1.1776$	0.5380
2	$T_5(H,O,S,E,T) = 0.4569$	$T_4^1(H,O,S,E) = 0.7129$	0.3257
3	$T_5(H,O,S,E,T) = 0.4569$	$T_4^2(H,O,S,T) = 0.6866$	0.3137
4	$T_5(H,O,S,E,T) = 0.4569$	$T_4^3(H,O,E,T) = 0.8154$	0.3726
5	$T_5(H,O,S,E,T) = 0.4569$	$T_4^4(H,S,E,T) = 0.5212$	0.2381
6	$T_5(H,O,S,E,T) = 0.4569$	$T_4^5(O,S,E,T) = 0.6174$	0.2821
7	$T_5(H,O,S,E,T) = 0.4569$	$T_3^1(H,O,S) = 0.2786$	0.1273
8	$T_5(H,O,S,E,T) = 0.4569$	$T_3^2(H,O,E) = 0.4839$	0.2211
9	$T_5(H,O,S,E,T) = 0.4569$	$T_3^3(H,O,T) = 0.3720$	0.1700
10	$T_5(H,O,S,E,T) = 0.4569$	$T_3^4(H,S,E) = 0.3217$	0.1470
11	$T_5(H,O,S,E,T) = 0.4569$	$T_3^5(H,S,T) = 0.1444$	0.0660
12	$T_5(H,O,S,E,T) = 0.4569$	$T_3^6(H,E,T) = 0.3961$	0.1810
13	$T_5(H,O,S,E,T) = 0.4569$	$T_3^7(O,S,E) = 0.1697$	0.0775
14	$T_5(H,O,S,E,T) = 0.4569$	$T_3^8(O,S,T) = 0.3528$	0.1612
15	$T_5(H,O,S,E,T) = 0.4569$	$T_3^9(O,E,T) = 0.2874$	0.1313
16	$T_5(H,O,S,E,T) = 0.4569$	$T_3^{10}(S,E,T) = 0.0623$	0.0285
17	$T_5(H,O,S,E,T) = 0.4569$	$T_2^1(H,O) = 0.1740$	0.0795
18	$T_5(H,O,S,E,T) = 0.4569$	$T_2^2(H,S) = 0.0032$	0.0015
19	$T_5(H,O,S,E,T) = 0.4569$	$T_2^3(H,E) = 0.2912$	0.1330
20	$T_5(H,O,S,E,T) = 0.4569$	$T_2^4(H,T) = 0.0324$	0.0148
21	$T_5(H,O,S,E,T) = 0.4569$	$T_2^5(O,S) = 0.0972$	0.0444
22	$T_5(H,O,S,E,T) = 0.4569$	$T_2^6(O,E) = 0.0085$	0.0039
23	$T_5(H,O,S,E,T) = 0.4569$	$T_2^7(O,T) = 0.0468$	0.0214
24	$T_5(H,O,S,E,T) = 0.4569$	$T_2^8(S,E) = 0.0047$	0.0021
25	$T_5(H,O,S,E,T) = 0.4569$	$T_2^9(S,T) = 0.0324$	0.0148
26	$T_5(H,O,S,E,T) = 0.4569$	$T_2^{10}(E,T) = 0.0013$	0.0006

4. Conclusion

Risk coupling analysis on ship accidents in port waters is important for navigational safety of out-or-in a port. In the case study, a ship navigating from the open sea to a berth in the west coast of Shenzhen port, China, is taken as example. The main findings of this research are as follows:

- Given a number of risk types in the sub-system of channel, the risk coupling value of the system decreases gradually as the number of risk types in the sub-system, i.e., berth, decreases.
- Particularly, when the number of risk types in the sub-system of berth involves two risk types, e.g., human and environment, the RCV of the whole system is larger than that when this sub-system involves three risk types, e.g., ship, environment, and technology.

In the future, a systematical framework could be developed in detail to incorporate the inherent uncertainty or to identify key sub-systems in the whole system.

Acknowledgements

This work is supported by funding from the National Natural Science Foundation of China (Grant No. 52301419, 52372416, 52001241), Fund of National Engineering Research Center for Water Transport Safety (Grant No. A202404). The views expressed remain solely those of the authors.

References

Aalberg, A.L., Bye, R.J., Ellevseth, P.R., 2022. Risk factors and navigation accidents: A historical analysis comparing accident-free and accident-prone vessels using indicators from AIS data and vessel databases. Maritime Transport Research 3, 100062.

Chen, J., Zhang, W., Song, L., Wang, Y., 2022. The coupling effect between economic development and the urban ecological environment in Shanghai port. Science of The Total Environment 841.

Fan, C.L., Montewka, J., Zhang, D., 2022a. A risk comparison framework for autonomous ships navigation. Reliability Engineering and System Safety 226, 108709.

Fan, L., Zhang, M., Yin, J., Zhang, J., 2022b. Impacts of dynamic inspection records on port state control efficiency using Bayesian network analysis. Reliability Engineering & System Safety 228.

Fu, G., Xie, X.C., Jia, Q.S., Li, Z.H., Chen, P., Ge, Y., 2020. The development history of accident causation models in the past 100 years: 24Model, a more modern accident causation model. Process Safety and Environmental Protection 134, 47–82.

Fu, Y., Lin, Q., Grifoll, M., Lee, L.J.S., Feng, H., 2023. Investigating the evolution of the Guangdong-Hong Kong-Macao Greater Bay Area (GBA) multi-port system: The multi-faced perspectives. Ocean and Coastal Management 233, 106450.

Gan, L., Che, W., Zhou, M., Zhou, C., Zheng, Y., Zhang, L., Rangel-Buitrago, N., Song, L., 2022. Ship exhaust emission estimation and analysis using Automatic Identification System data: The west area of Shenzhen port, China, as a case study. Ocean and Coastal Management 226, 106245.

Hua, W.Y., Chen, J.H., Qin, Q.D., Wan, Z., Song, L., 2021. Causation analysis and governance strategy for hazardous cargo accidents at ports case study of Tianjin ports hazardous cargo explosion accident. Marine Pollution Bulletin 173, 113053.

Kauffman, S.A., Weinberger, E.D., 1989. The NK model of rugged fitness landscapes and its application to maturation of the immune response. Journal of Theoretical Biology 141, 211–245.

Kong, Y., Liu, J., 2021. Sustainable port cities with coupling coordination and environmental efficiency. Ocean and Coastal Management 205, 105534.

Liu, K.Z., Yu, Q., Yang, Z.S., Wan, C.P., Yang, Z.L., 2022. BN-based port state control inspection for Paris MoU new risk factors and probability training using big data. Reliability Engineering and System Safety 224, 108530.

Ma, L., Ma, X., Liu, Y., Deng, W., Lan, H., 2023. Risk assessment of coupling links in hazardous chemicals maritime transportation system. Journal of Loss Prevention in the Process Industries 82.

Marineinsight, 2023. Container Ship Sinks Outside Kaohsiung Port In Taiwan.

Montewka, J., Manderbacka, T., Ruponen, P., Tompuri, M., Gil, M., Hirdaris, S., 2022. Accident susceptibility index for a passenger ship-a framework and case study. Reliability Engineering & System Safety 218.

Mou, J.M., Chen, P.F., He, Y.X., Yip, T.L., Li, W.H., Tang, J., Zhang, H.Z., 2019. Vessel traffic safety in busy waterways: A case study of accidents in western shenzhen port. Accident Analysis & Prevention 123, 461-468.

Qu, Y., Kong, Y., Li, Z., Zhu, E., 2023. Pursue the coordinated development of port-city economic construction. Ocean and Coastal Management 242, 106694.

Wang, L., Lau, Y.-y., Su, H., Zhu, Y., Kanrak, M., 2022. Dynamics of the Asian shipping network in adjacent ports: Comparative case studies of Shanghai-Ningbo and Hong Kong-Shenzhen. Ocean and Coastal Management 221, 106127.

Wang, Y., Zhang, F., Yang, Z., Yang, Z., 2021. Incorporation of deficiency data into the analysis of the dependency and interdependency among the risk factors influencing port state control inspection. Reliability Engineering & System Safety 206.

Yang, Z., Wan, C., Yang, Z., Yu, Q., 2021. dynamic port state control detention risk control decision. Reliability Engineering & System Safety 213.

Zhao, C., Yip, T.L., Wu, B., Lyu, J., 2022. Use of fuzzy fault tree analysis and Bayesian network for occurrence likelihood estimation of navigational accidents in the Qinzhou Port. Ocean Engineering 263.

Zhong, H., Chen, W., Gu, Y., 2023. A system dynamics model of port hinterland intermodal transport: A case study of Guangdong-Hong Kong-Macao Greater Bay Area under different carbon taxation policies. Research in Transportation Business & Management 49, 100987.